

TRANSIENT ANALYSIS OF A GAS-LIFT PRODUCTION SYSTEM USING A NON-ISOTHERMAL SIMPLIFIED DRIFT-FLUX MODEL

Eduardo Ferreira Gaspari

CENPES-PETROBRAS, Horácio de Macedo Avenue, 950, Rio de Janeiro-RJ, 21941-598, Brazil
eduardofgaspari@yahoo.com.br

Christiano Garcia da Silva Santim

CEPETRO-UNICAMP, Cora Coralina Street, 350, Campinas-SP, 13083-896, Brazil
christianosantim@gmail.com

Abstract. *The present study proposes a transient simulator able to reproduce important phenomena inherent to petroleum production systems based on the non-isothermal Drift-Flux model. The system of equations considers a three phase flow regardless the liquid-liquid drift velocity, assuming mass transfer among the phases and heat transfer counter-currently between gas injection and the production systems. Gas injection valves connecting service line and output line valves, important to system operation, as two master valves and surface choke besides of pumping facilities are also assumed in the mathematical formulation. The fluids' properties are estimated using a black oil model. The solver utilizes the finite volume method with a semi-implicit approach making use of the upwind first order scheme with staggered grid. Void fraction and liquid amount between the liquid phases are evaluated explicitly. The couple between velocities field and pressure is implicit by building a global matrix. It is not made an iterative process for the resolution of these fields. The temperature field is obtained in an uncoupled way after the volumetric fraction, mass flow rates and pressure calculus. Pressure, temperature and holdup trends are analyzed upstream and downstream of the master valve. The profiles of these interest variables as well as the superficial velocities along the production system are also reported showing that the thermal transient process is the slowest. This feature is due to the diffusive heat transfer in wall pipeline and in the well. The steep decay and the sudden increase of pressure at upstream and downstream regions, respectively, can result in operational problems depending on its magnitude.*

Keywords: *three phase flow, Drift-Flux model, gas-lift, non-isothermal, transient*

1. INTRODUCTION

It is known that the total reservoir volume is fixed and extremely depending on the rock formations of the corresponding area. As the reservoir fluid is produced, its pressure drops, causing the oil rate production diminishing. In this scenario, artificial lift methods are useful aiming to increase this previous oil rate production. Among these methods arises the gas-lift, which consists of a gas injection in a settle local in the tubing thereby aerating the fluid, thus reducing its density. The producing characteristics of the well that defines what type of gas-lift will be used. As advantages of this method can be cited the simplicity of the surface equipment for injection gas control requiring little maintenance and lower operation costs with compared against other methods of artificial lift.

There are two basic types of gas-lift in use today: continuous and intermittent flow (see Takacs (2005)). This work focus in the continuous gas-lift, which represents a good application for offshore formation. Its use is suitable for wells with productivity index higher than 1 and static pressure sufficient to support a fluid column in the range 40-70% of the total well depth (Gonzaga, 2009). The elevation making use of gas-lift has been extensively studied (Carrol, 1990; Ravindran, 1992; Ayatollahi *et al.*, 2005; Takacs, 2005; Ray and Sarker, 2007; De Souza *et al.*, 2010; Mahmudi and Sadeghi, 2013). The continuous gas-lift process may be divided into three operating modes: Normal operation state and the critical states known as shutdown and start-up. The shutdown commonly occurs after some operational problem in the process plant on the platform or to realize tests in order to obtain the Basic Sediment and Water (BSW), Gas-Oil Ratio (GOR), static pressure besides of the Inflow Performance Relationship (IPR) curve. The start-up procedure restarts the production line.

In particular, this work looks at the effect of a shutdown with a posterior start-up of petroleum production in a scenario similar to the pre-salt in deep water offshore Brazil presenting high static pressure of about 500kgf/cm² and a considerable CO₂ fraction, which not appears on the gas-lift.

2. MATHEMATICAL FORMULATION

The non-isothermal transient 1D gas-liquid-liquid flow is modeled based on the Drift-Flux model assuming mass transfer between the phases. The system of equations of the conservation laws is given by Eqs. (1)–(5) consisting of three mass conservation equations, being one for each phase, one momentum and one energy equation for the gas-liquid-liquid mixture.

Mass conservation of produced liquid

$$A \frac{\partial [\rho_{lp}(1-\alpha)(1-\beta)]}{\partial t} + \frac{\partial \dot{M}_{lp}}{\partial x} = \frac{\Gamma_{lp}}{\Delta L} - \psi \quad (1)$$

Mass conservation of conditioning liquid

$$A \frac{\partial [\rho_{lc}(1-\alpha)\beta]}{\partial t} + \frac{\partial \dot{M}_{lc}}{\partial x} = \frac{\Gamma_{lc}}{\Delta L} \quad (2)$$

Mass conservation of the gas phase

$$A \frac{\partial (\rho_g \alpha)}{\partial t} + \frac{\partial \dot{M}_g}{\partial x} = \frac{\Gamma_g}{\Delta L} + \psi \quad (3)$$

where α is the void fraction, β is the volumetric fraction of the conditioning fluid into the liquid mixture, ψ represents the mass transfer between the phases, Γ is the mass source term, L is a reference length, A is the cross sectional area, \dot{M} represents the mass flow rate with the subscripts lp , lc and g referring to the produced liquid, conditioning liquid and gas phases, respectively.

Momentum conservation of gas-liquid-liquid mixture

$$\frac{\partial \dot{M}_m}{\partial t} + \frac{\partial [u_l(\dot{M}_{lp} + \dot{M}_{lc}) + u_g \dot{M}_g]}{\partial x} + A \frac{\partial p}{\partial x} = f_m \frac{\rho_m j^2}{2} S_w + \rho_m g \sin(\theta) \quad (4)$$

in which u is velocity, p is the pressure, f represents the friction factor, ρ is the specific mass, g is the gravity acceleration, S_w is the wetted perimeter, θ is the tubing inclination, j is the volumetric flux and the subscript m refers to mixture.

Gas-liquid-liquid energy conservation

$$\begin{aligned} & \rho_g \alpha A \left[\frac{\partial \left(e_g + \frac{u_g^2}{2} \right)}{\partial t} + u_g \frac{\partial \left(h_g + \frac{u_g^2}{2} \right)}{\partial x} \right] + \rho_l (1-\alpha) A \left[\frac{\partial \left(e_l + \frac{u_l^2}{2} \right)}{\partial t} + u_l \frac{\partial \left(h_l + \frac{u_l^2}{2} \right)}{\partial x} \right] - \\ & \frac{Ap}{\rho_g} \left(\frac{\partial \rho_g}{\partial T} \frac{\partial T}{\partial t} + \frac{\partial \rho_g}{\partial p} \frac{\partial p}{\partial t} \right) = \\ & - \left(h_g + \frac{u_g^2}{2} \right) \frac{\Gamma_g}{\Delta L} - \left(h_l + \frac{u_l^2}{2} \right) \frac{\Gamma_{lp} + \Gamma_{cp}}{\Delta L} - \left(h_g - h_l + \frac{u_g^2}{2} - \frac{u_l^2}{2} \right) \psi - \\ & (\rho_g u_g \alpha_g) Ag - \rho_l u_l (1-\alpha) Ag + Q_w + \frac{h_{Fg} \Gamma_g}{\Delta l} + \frac{(h_{Flp} \Gamma_{lp} + h_{Flc} \Gamma_{lc})}{\Delta l} - \\ & \frac{A}{\rho_l} p (1-\alpha) (\rho_{lc} - \rho_{lp}) \frac{\partial \beta}{\partial t} \end{aligned} \quad (5)$$

where e is the internal energy, h is the enthalpy, the source term Q_w represents the heat flux and the subscripts l , Fg , Flp and Flc refer to the liquid-liquid mixture and the enthalpy sources for each phase separately.

To solve the system above, the closure law presented by Zuber and Findlay (1965) is used,

$$u_g = C_0 j + u_d \quad (6)$$

in which u_d is the drift velocity. The parameters C_0 and u_d are defined accordingly to the fluids transport properties and by the flow pattern.

The gas-liquid-liquid mixture properties are defined as follows:

Specific mass of the liquid-liquid mixture

$$\rho_l = (1 - \beta)\rho_{lp} + \beta\rho_{lc} \quad (7)$$

Specific mass of the gas-liquid-liquid mixture

$$\rho_m = (1 - \alpha)\rho_l + \alpha\rho_g \quad (8)$$

Dynamic viscosity of the liquid-liquid mixture

$$\mu_l = (1 - \beta)\mu_{lp} + \beta\mu_{lc} \quad (9)$$

Dynamic viscosity of the gas-liquid-liquid mixture

$$\mu_m = (1 - \alpha)\mu_l + \alpha\mu_g \quad (10)$$

The mass transfer rate between the phases is given by Eq. (11) making use of relations for the fluid properties inherent to black oil models. This work assumes two phases for the black oil model: liquid phase (oil+dissolved gas) and gas phase.

$$\psi = -A \frac{\partial \left[(1 - \alpha)(1 - \beta)(1 - F_w) \frac{R_s \gamma_g \rho_{ar}^{std}}{B_o} \right]}{\partial t} - \frac{\partial \left[(1 - \beta)(1 - F_w) \frac{R_s \gamma_g \rho_{ar}^{std}}{B_o} Q_l \right]}{\partial x} \quad (11)$$

where R_s represents the solution gas-oil ratio (or GOR of production), B_o is the formation volume factor, γ_g is the gas density, ρ_{ar}^{std} represents the specific mass of air at standard conditions whereas Q_l is the liquid-liquid mixture flow rate. The water fraction into the produced liquid (F_w), excluding the possibility of gas dissolved in water, is represented by

$$F_w = \frac{F_w^{std}}{B_o + F_w^{std} - F_w^{std} B_o} \quad (12)$$

in which F_w^{std} is the water fraction on the liquid phase at standard conditions. When sediments are not assumed its value is equal to the BSW.

The R_s and B_o calculus are done making use the correlations presented previously by Vazquez and Beggs (1980). The temperature and pressure pseudocritical values, T_c and p_c , are obtained by Piper *et al.* (1993) considering corrections for high CO₂ concentration. The oil viscosity is calculated using Glaso (1980) relations. For cases with emulsion, the oil viscosity is obtained from Woelflin (1942). The instantaneous GOR is estimated through Eq. (13).

$$GOR = \frac{Vol_{gas} B_o}{(1 - \alpha)(1 - \beta)(1 - F_w) A} \quad (13)$$

where the light volume represented by Vol_{gas} is given as

$$Vol_{gas} = A \left[(1 - \alpha)(1 - \beta)(1 - F_w) \frac{R_s}{B_o} + \alpha \frac{\rho_g}{\rho_g^{std}} \right] \quad (14)$$

3. NUMERICAL MODEL

The solver utilizes the finite volume method with a semi-implicit approach making use of the upwind first order scheme with staggered grid. Void fraction (α) and liquid amount among the liquid phases (β) are evaluated explicitly. The couple between velocities and pressure fields is implicit by building of a global matrix (\mathbf{A}). It is not made an iterative process for the resolution of these fields which are solved as $\mathbf{A}\mathbf{X}=\mathbf{B}$ by Gauss elimination with partial pivoting (\mathbf{A} is the coefficient matrix, \mathbf{B} is a right side vector and \mathbf{X} are the primitive variables to be calculated). The temperature field is obtained in an uncoupled way after the volumetric fraction, mass flow rates and pressure calculus.

The global matrix is of band type. Two local matrices (related to the cells i and $i+1$) presenting 2 lines and 8 columns are necessary to build the global matrix. The first line of local matrix arises from the G-L-L mixture mass conservation equation whereas the second line is obtained from the G-L-L mixture momentum equation. So, the 1st (cell i) and 3rd (cell $i+1$) lines of the global matrix are related with the mixture mass conservation and the 2nd (cell i) and 4th (cell $i+1$) lines with the mixture momentum equation, as

$$\mathbf{A} = \begin{bmatrix} \vdots \\ \text{local}_{\text{cell } i} \\ \text{local}_{\text{cell } i+1} \\ \vdots \end{bmatrix} = \begin{bmatrix} [0,0] & [0,1] & [0,2] & 0_{0x3} & 0_{0x4} & 0 & 0 & 0 \\ 0 & 0_{1x0} & 0_{1x1} & [1,2] & [1,3] & [1,4] & 0 & 0 \\ 0 & 0 & [0,0] & [0,1] & [0,2] & 0_{0x3} & 0_{0x4} & 0 \\ 0 & 0 & 0 & 0_{1x0} & 0_{1x1} & [1,2] & [1,3] & [1,4] \\ \vdots \end{bmatrix}_{i+1} \quad (15)$$

The primitive variables to be solved, the G-L-L mass flow rate and the absolute pressure, are always represented by the main diagonal (in red color) of the global matrix.

As example of the discretization is presented hereafter the 1st line of the local matrix (cell i) and its right side vector term (for more details, see Gaspari (2015)).

$$\begin{aligned} & \underbrace{\left[-\frac{1}{\rho_m} \Big|_{i-1}^n \frac{T_1 \Big|_{i-1}^n}{\Delta x_{i-1}} - \frac{1}{\rho_g} \Big|_{i-1}^n \frac{(1-T_1 \Big|_{i-1}^n)}{\Delta x_{i-1}} \right]}_{A[0,0]} \dot{M}_m \Big|_{i-1}^{n+1} + \underbrace{\frac{1}{\Delta t} \left(\frac{\alpha A}{\rho_g} \frac{\partial \rho_g}{\partial p} \right) \Big|_{i-1}^n}_{A[0,1]} p \Big|_{i-1}^{n+1} + \\ & \underbrace{\left[\frac{1}{\rho_m} \Big|_{i-1}^n \frac{T_1 \Big|_i^n}{\Delta x_i} + \frac{1}{\rho_g} \Big|_{i-1}^n \frac{\left((1-T_1 \Big|_i^n) \right)}{\Delta x_i} \right]}_{A[0,2]} \dot{M}_m \Big|_i^{n+1} = \\ & \frac{1}{\Delta t} \left(\frac{\alpha A}{\rho_g} \frac{\partial \rho_g}{\partial p} \right) \Big|_{i-1}^n p \Big|_{i-1}^n - \frac{1}{\rho_m} \Big|_{i-1}^n \frac{T_2 \Big|_i^n - T_2 \Big|_{i-1}^n}{\Delta x_{i-1}} + \frac{1}{\rho_g} \Big|_{i-1}^n \frac{T_2 \Big|_i^n - T_2 \Big|_{i-1}^n}{\Delta x_{i-1}} - \\ & \left(\frac{A(\rho_{lc} - \rho_{lp})(1-\alpha)}{\rho_m} \right) \Big|_{i-1}^n \frac{\beta_{i-1}^{n+1} - \beta_{i-1}^n}{\Delta t} + \left[\left(\frac{1}{\rho_g} - \frac{1}{\rho_m} \right) \Big|_{i-1}^n \Psi \Big|_{i-1}^n \right] + \\ & \underbrace{\left[\frac{\Gamma_{lp}}{\rho_m \Delta x} \Big|_{i-1}^n + \frac{\Gamma_{lc}}{\rho_m \Delta x} \Big|_{i-1}^n + \frac{\Gamma_g}{\rho_g \Delta x} \Big|_{i-1}^n \right]}_{B[0]} \end{aligned} \quad (16)$$

where T_1 and T_2 are given by Eqs. (17) and (18) respectively.

$$T_1 = \frac{1 - \alpha C_0}{1 - \alpha C_0 \left(1 - \frac{\rho_g}{\rho_l} \right)} \quad (17)$$

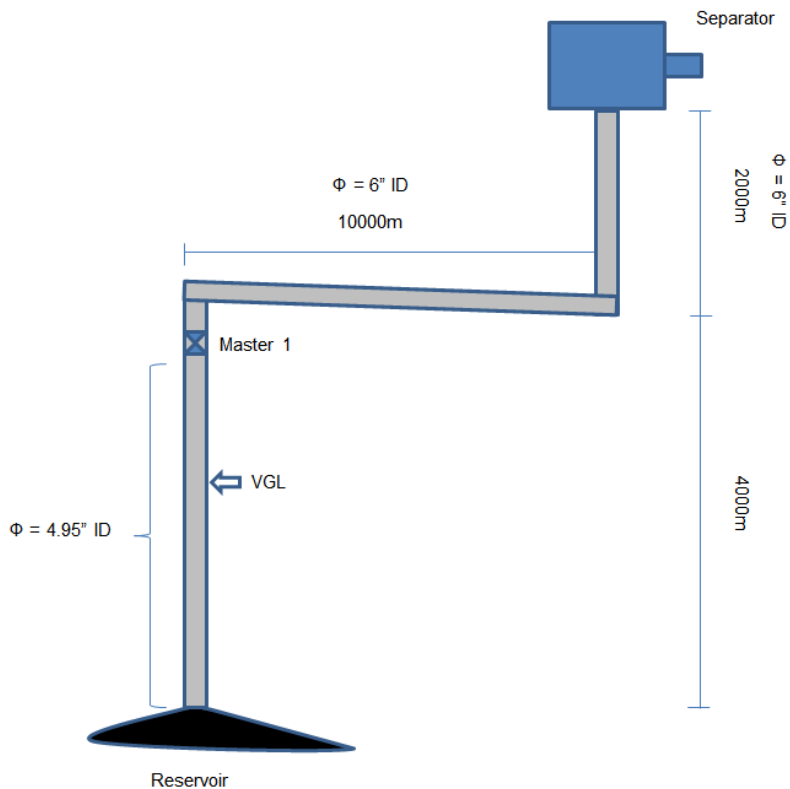
$$T_2 = - \frac{\alpha A u_d \rho_g}{1 - \alpha C_0 \left(1 - \frac{\rho_g}{\rho_l} \right)} \quad (18)$$

The auxiliary variables T_1 and T_2 come from the relation

$$\dot{M}_l |^{n+1} = \left[\frac{1 - \alpha C_0}{1 - \alpha C_0 \left(1 - \frac{\rho_g}{\rho_l} \right)} \right]^n \dot{M}_m |^{n+1} + \left[\frac{\alpha A u_d \rho_g}{1 - \alpha C_0 \left(1 - \frac{\rho_g}{\rho_l} \right)} \right]^n \quad (19)$$

4. NUMERICAL PROCEDURE

The test section, presented in Fig. 1, represents the production line which has a vertical well with 4km long and 4.95" ID, a flexible pipeline of 10km long and 6" ID inclined by -2° and 2km of riser with the same internal diameter of 6", totaling 16km. The master 1 valve is located at 3960m upward to the bottom well. The gas pipeline follows the production line with 4" ID, being annular to the well, with an internal and external diameter of 5.5" and 8.5" respectively. The master 2 valve is disposed at the same position of master 1. The gas-lift orifice valve (0.375") is placed 2820m above the well bottom presenting a flow rate of $150000 \text{ Sm}^3/\text{d}$. The injected gas has a density of 0.55.



3960

Figure 1. Sketch of the production line.

The reservoir (Productivity index=100, static pressure= 500 kgf/cm^2 , API=32, GOR= $400 \text{ Sm}^3/\text{Sm}^3$, Y_{CO_2} =0.44, BSW=0.5 and gas formation density of 1.1) is treated as a mass source applied to the first cell and is represented by an IPR Vogel's type assuming a linear correction for bottom pressures higher than the saturation.

The separator pressure is assumed to be 10 kgf/cm^2 .

The proposed problem presents characteristics resembling to the pre-salt scenario and was chosen aiming to assess the simulator robustness as well as its ability to represent industrial operations inherent to the petroleum elevation and production (high static pressure, GOR and CO₂ percentage).

The numerical simulation starts making use of initial conditions too far from the correct steady-state. So the initial steady-state of the numerical solution occurs after 50000s. Thenceforward, the master valves and the choke are closed, characterizing a shutdown. After 1000s the choke valve is partially opened aiming to depressurize the system. Afterward 8000s with the production interrupted, starts a conditioning procedure of the production line injecting ethanol (2000 Sm³/d during 1000s). Then, a pig (inserted downstream of master 1 valve in $t=64100s$) will push all phases to out of the system, through a gas injection of 300000 Sm³/d. When the system achieves low pressure, the start-up procedure is initialized with the master and gas-lift valves aperture. The simulation reaches the final steady-state after 30000s from the start-up.

5. RESULTS AND DISCUSSION

Figure 2 shows the trends of pressure (a), temperature (b) and holdup (c) upstream to master 1 valve whereas Fig. 3 presents these transient behaviors at downstream.

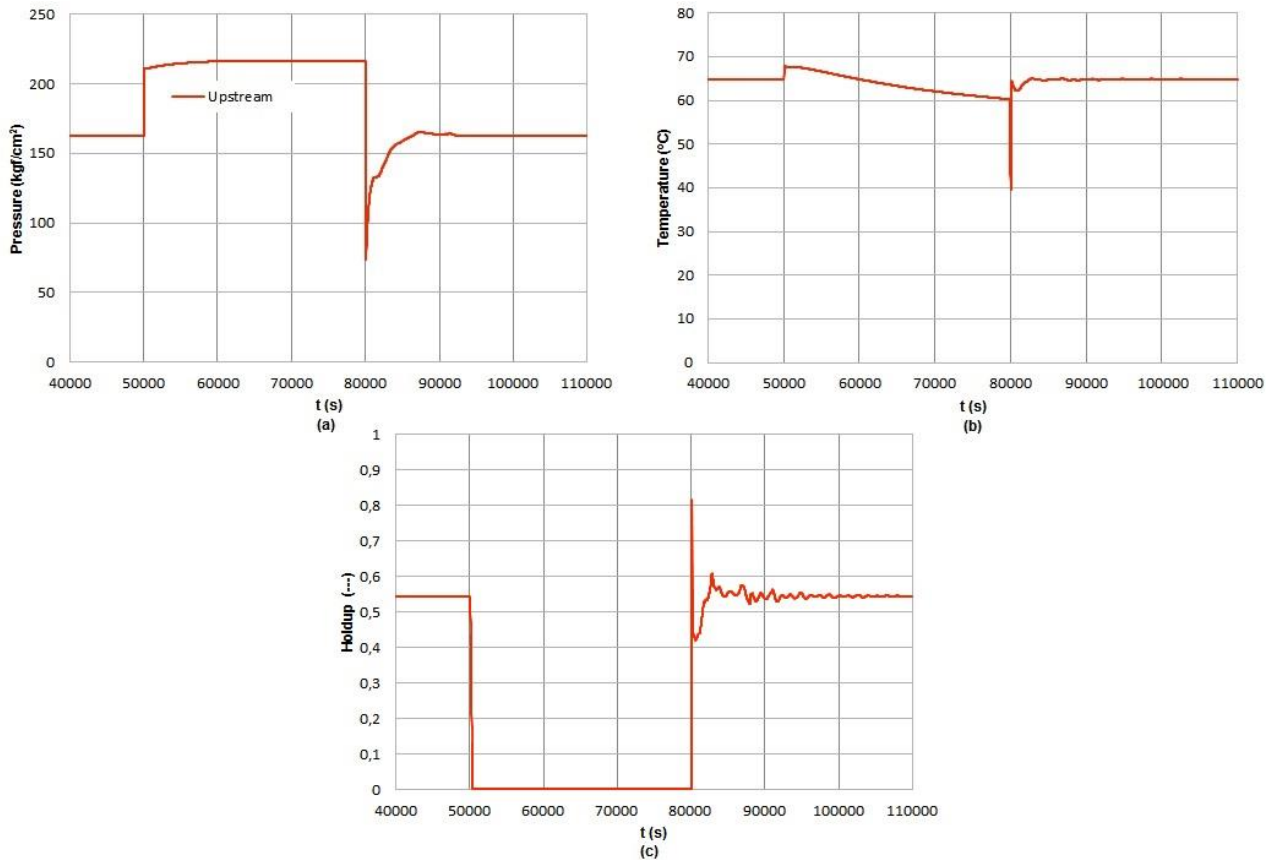


Figure 2. Transient behavior upstream of master 1. (a) pressure; (b) temperature; (c) liquid holdup, $(1-\alpha)$.

By analysis of Figs 2 and 3, the final steady-state is reached in around 30000s after the start-up ($t_{start-up}=80000s$). Upstream of the master 1 valve, after the master 1 closure, it is possible to verify a gradual pressure increase. It is the shut in pressure due to the reservoir pressure. On the other hand, downstream the master 1, it is observed a pressure decrease until about $t=55000s$, due to the fluid segregation and an open choke on the surface. The liquid holdup downstream of the master 1 goes to zero caused by the pipeline inclination (-2 degree), in the same way, the liquid holdup upstream goes to zero after the master 1 closure. In $t=58000s$ is injected ethanol during 1000s with a volumetric flow rate of 2000 Sm³/d. A pig is then applied into the system in $t=64100s$. These last procedures that cause the transient behavior in the range between 58000-80000s. In this interval is observed three peaks of pressure induced by three liquid pocket discharges that can be seen in Fig. 4.

Figure 5 exhibits the pressure, temperature and liquid holdup trends 40m above the reservoir.

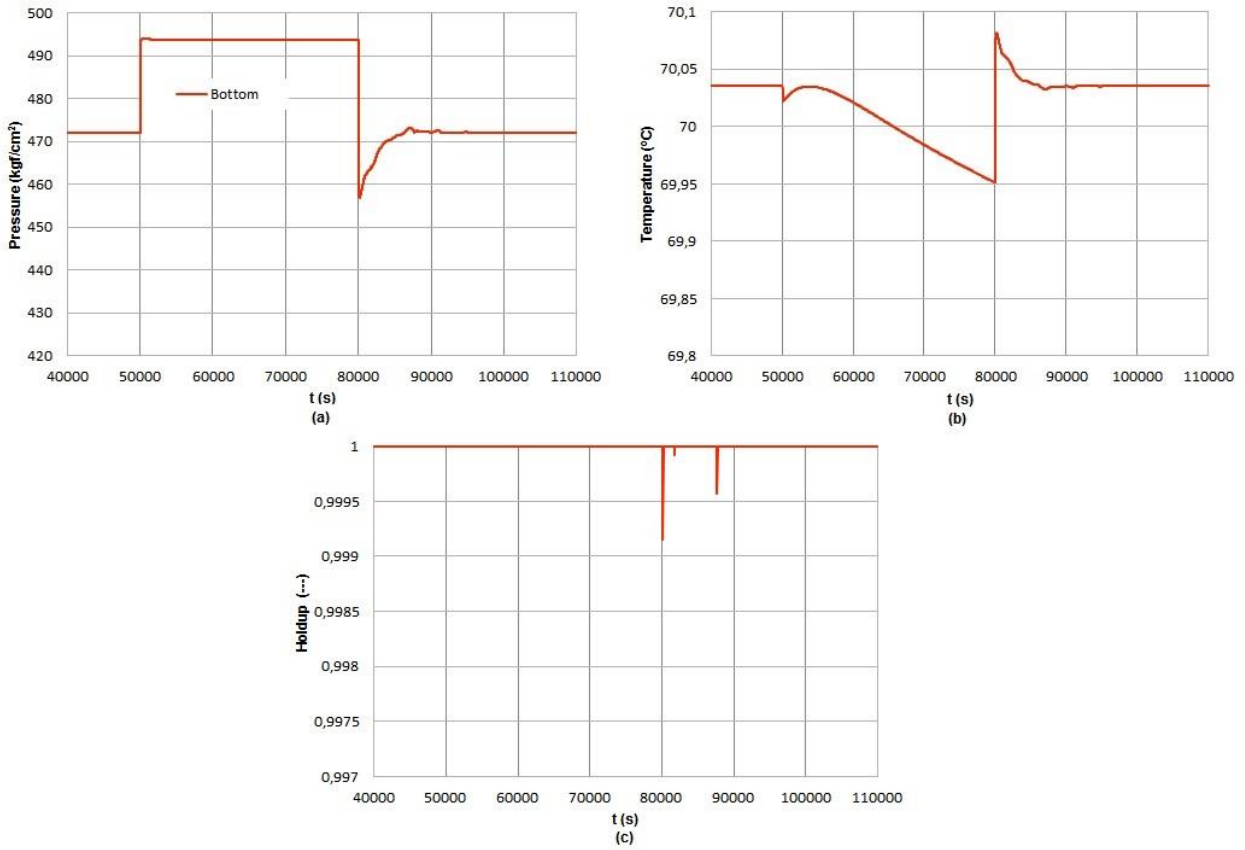


Figure 5. Transient behavior at the well bottom ($x=40\text{m}$). (a) pressure; (b) temperature; (c) liquid holdup.

Through analysis of the Fig. 5 it can be qualitatively noted a similar pressure behavior with the solution upstream to the master 1 valve. Quantitatively, it is observed that at the well bottom region, the magnitude is considerably lower. The liquid holdup as well as the temperature practically does not change. At these conditions of pressure and temperature, the gas stays almost totally dissolved in the oil.

The transient behavior near to the outlet region is provided by the Fig. 6. Through analysis of Fig. 6a, it can be noted the pressure peaks damped. On the other hand, in Fig. 6b is observed large amplitude (about 110°C) inherent to the temperature variation. From Fig. 6c it is clear the occurrence of gas plugs.

Figure 7 provides the pressure, temperature, holdup and the superficial velocities profiles along the production line in the final steady-state ($t=110000\text{s}$). As it can be seen through Fig. 7a, the pressure varies from 500 to 10kgf/cm^2 , decreasing more abruptly in the well section (approximately 0.1kgf/m) whereas the temperature (Fig. 7b) faster decays in the raiser section (about 0.008°C/m). The superficial velocity of the gas phase (Fig. 7d) increases along the production line presenting higher values than the liquid (Fig. 7c) starting from the head well. From Fig. 7e, it can be noted three different flow patterns: single phase flow (liquid phase), bubble and slug, with the intermittent flow pattern appearing in the lasts 12km of the production line.

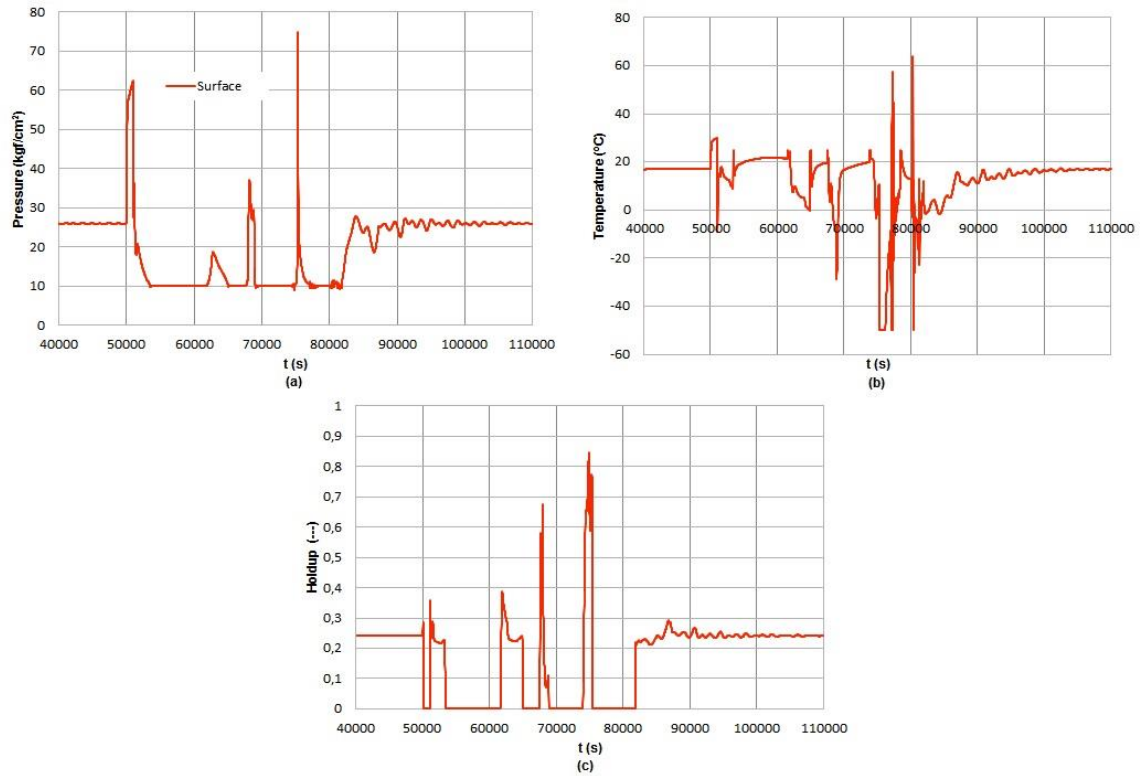


Figure 6. Numerical trends in $x=15.960\text{km}$. (a) pressure; (b) temperature; (c) liquid holdup.

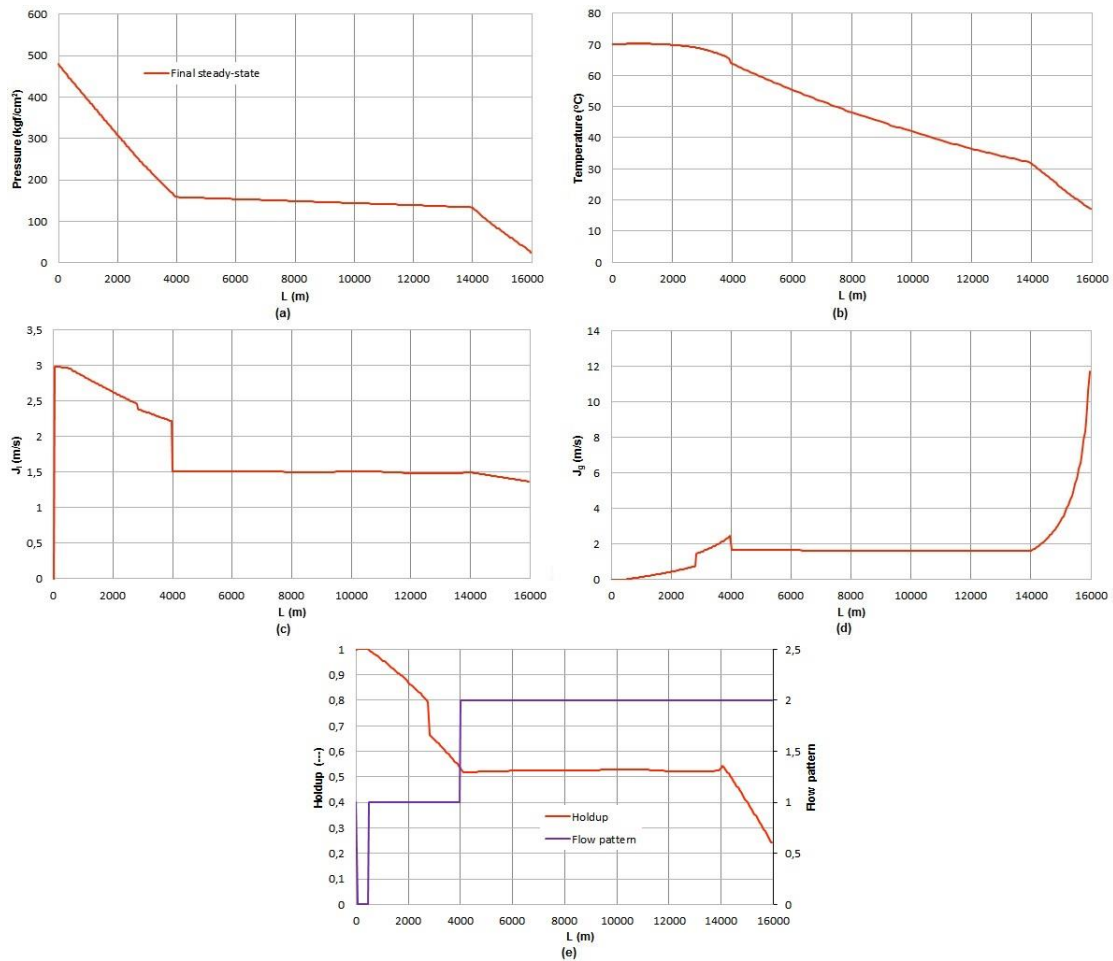


Figure 7. Numerical solution along the production line at the final steady-state. (a) pressure; (b) temperature; (c) liquid superficial velocity; (d) gas superficial velocity; (e) holdup/flow patterns.

6. SUMMARY AND CONCLUSIONS

A non-isothermal transient 1D simulator based on the finite volume method using the Drift-Flux model is presented. The transient simulator is tested in a problem resembling to the pre-salt scenario, using continuous gas-lift aiming to guarantee the elevation of the oil. The transients analyzed are caused by shutdown and start-up procedures in an extensive production line. The main conclusions are drawn as follow:

The shutdown causes an abrupt increase of pressure at the upstream of master 1 valve that must be assumed on the tubing project thereby avoiding potential damages.

The displacement of the ethanol package injected into the production line aiming to prevent the formation of hydrates can cause extreme events in the process plant when the pig reaches the platform. The pig passage cleans the line production thereby reducing the pressure downstream to master 1 valve.

The start-up process shows to be the main critical moment. Pressure, temperature and liquid holdup sudden increase or decay its values, presenting significant amplitude may causing operational problems. This behavior is explained by the substantial difference between the pressure immediately to upstream and downstream of the master 1 valve, represented by approximately 200kgf/cm^2 .

The proposed transient simulator exhibits great robustness since it presents consistent results in a complex industrial problem inherent to the offshore oil & gas production.

7. ACKNOWLEDGEMENTS

The authors acknowledge the financial support from PETROBRAS under contract number 0050-0099955.16.9.

8. REFERENCES

- Ayatollahi, S., Tauseef, S.M., Guzman, C., 2005. Compositional model optimizes gas lift, *Oil Gas J*, January, p. 37-42.
- Carrol, J.A., 1990. *Multivariate production systems optimization*, Ph.D. thesis, Stanford, USA.
- Choi, J., Pereyra, E., Sarica, C., Park, C., Kang, J.M., 2012. An efficient drift-flux closure relationship to estimate liquid holdups of gas-liquid two-phase flow in pipes, *Energies* 5, Vol. 12, p. 5294-5306.
- França, H., Lahey Jr, R.T., 1992. The use of drift flux techniques for the analysis of horizontal two phase flows, *Int. J. Multiph. Flow*, Vol. 18, p. 787-801.
- Gaspari, E.F., 2015. Módulo transiente do simulador MARLIM (modelo hidrodinâmico), relatório técnico, CENPES/PDP/TEE.
- Glaso, Ø., 1980. Generalized pressure-volume-temperature correlation, *J. Petroleum Tech.*, p. 785-795.
- Gonzaga, C.A.C., 2009. *Uma proposta para o controle automático da repartida de poços operando por gas lift contínuo*, Ph.D. thesis, Florianópolis, Brazil.
- Hibiki, T., Ishii, M., 2003. One-dimensional drift flux model and constitutive equations for relative motion between phases in various two-phase flow regimes, *Int. J. Heat Mass Transf.*, Vol. 46, p. 4935-4948.
- Mahmudi, M., Sadeghi, M.T., 2013. The optimization of continuous gas lift process using an integrated compositional model, *J. Pet. Sci. Eng.*, Vol. 108, August, p. 321-327.
- Piper, L.D., McCain Jr., S.A., Corredor, J.H., 1993. Compressibility factors for naturally occurring petroleum gases. Presented at the 68th Annual Tech. Conf. and Exhibit., SPE, Houston, (SPE n° 26668).
- Ravindran, N., 1992. *Multivariate optimization of production systems-the time dimension*, Ph.D. thesis, Stanford, USA.
- Ray, T., Sarker, R., 2007. Genetic algorithm for solving a gas lift optimization problem, *J. Pet. Sci. Eng.*, Vol. 59, p. 84-96.
- De Souza, J.N.M., de Medeiros, J.L., Costa, A.L.H., Nunes, G.C., 2010. Modelling, simulation and optimization of continuous gas lift systems for deepwater offshore petroleum production, *J. Pet. Sci. Eng.*, Vol. 72, n. 3-4 (June), p. 277-289.
- Takacs, G., 2005. *Gas Lift Manual*. PennWell Corporation, Tulsa.
- Vazquez, M., Beggs, H.D., 1980. Correlations for fluid physical property prediction, *J. Petroleum Tech.*, p. 968-970.
- Zuber N., Findlay J.A., 1965. Average volumetric concentration in two-phase flow systems. *Journal of Heat Transfer-Transactions of the ASME*, Vol. 87, p. 453-468.
- Woelflin, W., 1942. The viscosity of crude-oil emulsions. Presented at the API Drilling and Production Practice Conference, New York. API-42-148.

9. RESPONSIBILITY NOTICE

The authors are the only responsible for the printed material included in this paper.